Chemical Science

Accepted Manuscript

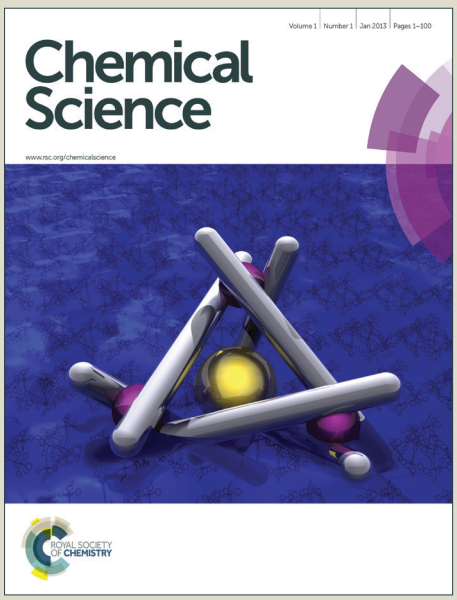

ROYAL SOCIETY OF CHEMISTRY

www.rsc.org/chemicalscience

Chemical Science

RSCPublishing

EDGE ARTICLE

Antiaromatic Bisindeno-[*n*]thienoacenes With Small Singlet Biradical Characters: Syntheses, Structures and Chain Length Dependent Physical Properties

Cite this: DOI: 10.1039/x0xx00000x

Received 00th January 2012,
Accepted 00th January 2012

DOI: 10.1039/x0xx00000x

www.rsc.org/

Xueliang Shi,[a] Paula M. Burrezo,[b] Sangsu Lee,[c] Wenhua Zhang,[d] Bin Zheng,[e] Gaole Dai,[a] Jingjing Chang,[a] Juan T. López Navarrete,[b] Kuo-Wei Huang,*[,e] Dongho Kim,*[,c] Juan Casado,*[,b] and Chunyan Chi*[,a]

Recent studies demonstrated that aromaticity and biradical character played important roles on determining the ground-state structures and physical properties of quinoidal polycyclic hydrocarbons and oligothiophenes, a kind of molecular materials showing promising applications for organic electronics, photonics and spintronics. In this work, we designed and synthesized a new type of hybrid system, the so-called bisindeno-[*n*]thienoacenes (n = 1-4), by annulation of quinoidal fused α-oligothiophenes with two indene units. The obtained molecules can be regarded as antiaromatic systems containing 4*n* π electrons with small singlet biradical characters (y_0). Their ground-state geometry and electronic structures were studied by X-ray crystallographic analysis, NMR, ESR and Raman spectroscopy, assisted by density functional theory calculations. With extension of the chain length, the molecules showed a gradual increase of the singlet biradical character accompanying with decreased antiaromaticity, finally leading to a highly reactive bisindeno[4]thienoacene (**S4-TIPS**) which has a singlet biradical ground state (y_0 = 0.202). Their optical and electronic properties in the neutral and charged states were systematically investigated by one-photon absorption, two-photon absorption, transient absorption spectroscopy, cyclic voltammetry and spectroelectrochemistry, which could be correlated to the chain length dependent antiaromaticity and biradical character. Our detailed studies revealed a clear structure-aromaticity-biradical character-physical properties-reactivity relationship, which is of importance for tailored material design in the future.

Introduction

Quinoidal π-conjugated structures are fundamentally important for organic optical, electronic and magnetic materials as they are closely related to the doped state of semiconducting polymers.[1] Recent studies demonstrated that quinoidal polycyclic hydrocarbons (PHs)[2] and oligothiophenes[3] could show obvious singlet biradical character and unique optical, electronic and magnetic activity, which lead to versatile applications for organic electronics,[4] non-linear optics,[5] organic spintronics,[6] organic photovoltaics[7] and energy storage devices.[8] The fundamental subunits of the quinoidal PHs are pro-aromatic *p*-quinodimethane (*p*-QDM, **1**), 2,6-naphthoquinodimethane (**2**), 2,6-anthraquinodimethane (**3**), and their isomers, which are embedded into an aromatic framework (Fig. 1). By using different fusion motifs, various quinoidal PHs have been designed and synthesized, and typical examples are bisphenalenyls (e.g. **4**) reported by Kubo *et al*.,[9] indenofluorenes (e.g. **5**) reported by Haley and Tobe *et al*.,[10] zethrenes (e.g. **6**)[11] and extended *p*-QDMs[12] reported by Wu *et al*. (Fig. 1). Some of this type of hydrocarbons showed significant biradical character in the ground state due to recovery of the aromaticity of the pro-aromatic quinodimethanes in the biradical resonance form. As a consequence, their physical properties are distinctly different from the traditional closed-shell PHs. Similarly, quinoidal oligothiophenes (**7**)[3] have been intensively studied due to the unique magnetic activity for higher order oligomers[13] and their promising applications for ambipolar and *n*-channel organic field effect transistors (OFETs).[14] In addition, fused *α*-oligothiophenes and thiophene-fused acenes, the so-called thienoacenes, have been demonstrated to be excellent organic semiconductors for OFETs by Takimiya *et al*..[15] Their quinoidal counterparts, the [*n*]thienoacenequinodimethanes (**8**) thus are of interest. However, synthesis of such type of molecules are challenging due to the lack of efficient synthetic method and their poor solubility.[16] Incorporation of these subunits into a polycyclic hydrocarbon framework is supposed to lead to new hybrid systems with unique physical properties but it becomes even more challenging. To the best of our knowledge, no such kind of research work has been reported. In this context, we are particularly interested

in the bisindeno-[*n*]thienoacenes **9-12** (n = 1-4), in which a quinoidal thienoacene unit is annulated with two indene rings (Fig. 1).

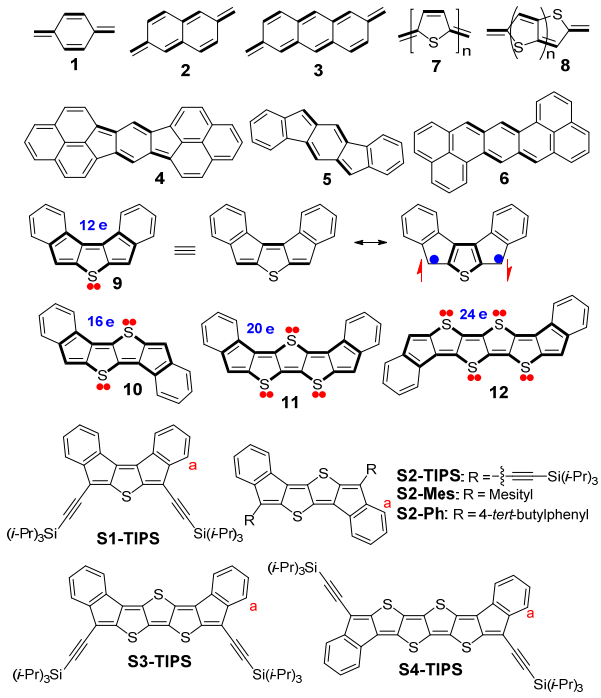

Fig. 1. Fundamental quinodimethanes and representative quinoidal hydrocarbons and bisindeno-[*n*]thienoacenes.

Similar to the quinoidal oligothiophenes, significant contribution of the biradical resonance form to their ground-state structures can be expected due to the recovery of the aromaticity of the fused thiophene rings. Looking into the structures from another angle, this type of molecules can be regarded as dibenzannulated antiaromatic systems containing 4*n* π electrons (highlighted in bold form in Fig. 1) if two π electrons are counted for each sulfur atom. It is well known that antiaromatic systems, regarding their aromatic analogues, have a pair of electrons in defect (i.e., 4*n* versus 4*n*+2) that transforms the ground electronic state from an in-phase stabilizing combination of Kekulé structures for the aromatics into an out-of-phase combination which originates the antiaromatic unstability. In order to mitigate such unstabilization, the highest energy bounded 4*n* electron pair might lead to the formation of a biradical if these two electrons are uncorrelated (in large size systems). Such interesting structural features imply their unique physical properties related to their biradical character and antiaromaticity, as well as their interdependence or interconversion as a function of the chain length. Therefore, our particular interests of this work include: (1) their efficient synthesis; (2) their geometry and electronic structures in the ground state; (3) their chain length dependent optical, electronic and magnetic properties. In addition, the properties of their charged forms are also of interest because of the change of aromaticity upon gain or loss of one or two π electrons. Such fundamental studies will help us to better understand the role of aromaticity and biradical character on the physical properties of quinoidal systems and allow us to do tailored design in the future.

The parent compounds **9-12** are predicted to be unstable due to the contribution of the biradical resonance form to the ground-state structures and they are also insoluble. Therefore, their derivatives in which the most reactive sites are kinetically blocked by triisopropylsilylethynyl (TIPSE) group (**S1-TIPS**, **S2-TIPS**, **S3-TIPS**, **S4-TIPS**) or aryl groups (**S2-Mes**, **S2-Ph**) (Fig. 1) were designed and synthesized. Their ground-state geometry and electronic structures were investigated by X-ray crystallographic analysis, NMR, ESR and Raman spectroscopy, assisted by density functional theory (DFT) calculations. Their physical properties were systematically studied by different experimental techniques, including one-photon absorption (OPA), transient absorption (TA), two-photon absorption (TPA), Raman spectroscopy, cyclic voltammetry, and spectroelectrochemistry. The properties were rationally correlated to the chain length dependent antiaromaticity and biradical character in this unique quinoidal and antiaromatic system.

Results and discussion

Synthesis

The synthetic methodology used to synthesize substituted acenes,[17] indenofluorenes[10] and zethrenes[11] was utilized to obtain our target compounds. That is, the corresponding diketones were prepared first, followed by nucleophilic addition with lithiated TIPSE or aryl groups, and then by reduction of the intermediate diols with $SnCl_2$. The major challenge was the synthesis of the bisindeno-thienoacene diketones, which were achieved by different strategies.

The synthesis of **S1-TIPS** commenced with Knoevenagel type condensation reaction between diethyl thiodiglycolate (**13**) and benzil (**14**) under strong basic conditions according to a published procedure with minor modification, giving the 3,4-diphenylthiophene-2,5-dicarboxylic acid (**15**) in 60% yield (Scheme 1).[18] The diacid **15** was then treated with an excess of thionyl chloride to afford the 3,4-diphenylthiophene-2,5-dicarbonyl chloride, and subsequent double Friedel–Crafts acylation with $AlCl_3$ gave the desired diketone **16** in 85% yield. Compound **S1-TIPS** was then obtained as a dark green solid in an overall 70% yield by addition of lithiated TIPSE to the diketone **16** followed by reductive dehydroxylation with $SnCl_2$.

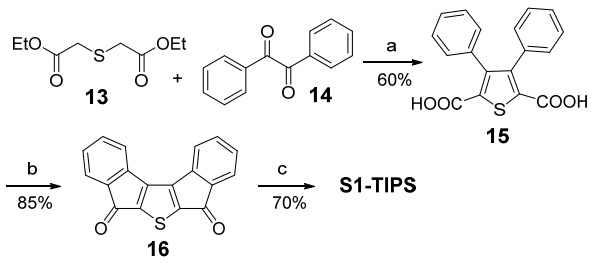

Scheme 1. Synthetic route of **S1-TIPS**: (a) i) CH_3ONa, EtOH, r.t. for 4 h and then 60 °C for 12 h; ii) NaOH, EtOH, reflux, 12 h; iii) 10% HCl (aq.); (b) i) $SOCl_2$, CH_2Cl_2, reflux; ii) $AlCl_3$, CH_2Cl_2, 0 °C – r.t., 12 h; (c) i) TIPSC≡CLi, THF, r.t., 12h; ii) $SnCl_2$, toluene, r.t., 12 h.

The synthesis of compounds **S2-TIPS**, **S2-Mes** and **S2-Ph** are outlined in Scheme 2. Three different substituents (TIPSE, mesityl and 4-*tert*-butylphenyl) are introduced to investigate the effect of the substituent on the physical properties. The starting compound is 2,3,5,6-tetrabromothieno[3,2-b]thiophene **17**, which was prepared according to reported procedure.[19] Based on our previous work, the key intermediate **18** was obtained in 70% yield by selective introduction of two ester groups to the α-positions of **17**.[20] Suzuki coupling reaction between **18** and phenylboronic acid gave **19** in 94% yield. Hydrolysis of **19** produced the diacid **20** which was treated with $SOCl_2$ and then $AlCl_3$ to give the desired diketone **21** in an overall 80% yield. Subsequent addition of lithiated regents and reduction of the intermediate diols by $SnCl_2$ gave **S2-TIPS**, **S2-Mes** and **S2-Ph** in 70%, 50%, and 40% yield, respectively.

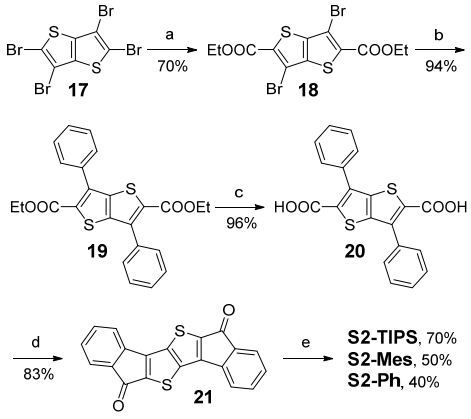

Scheme 2. Synthetic route of **S2-TIPS**, **S2-Mes** and **S2-Ph**: (a) i) *n*-BuLi, THF, -78 °C, 1h; ii) NC-COOEt, -78 °C – r.t., overnight; (b) $PhB(OH)_2$, $Pd(PPh_3)_4$, Na_2CO_3, toluene/H_2O, reflux, 12 h; (c) NaOH, MeOH/THF (1:1), reflux, overnight; (d) i) $SOCl_2$, CH_2Cl_2, reflux, overnight; ii) $AlCl_3$, CH_2Cl_2, 0 °C – r.t., overnight; (e) i) TIPSC≡CLi, or Mes-MgBr or 4-*tert*-butylphenylLi, 0 °C – r.t., overnight; ii) $SnCl_2$, toluene, r.t., overnight.

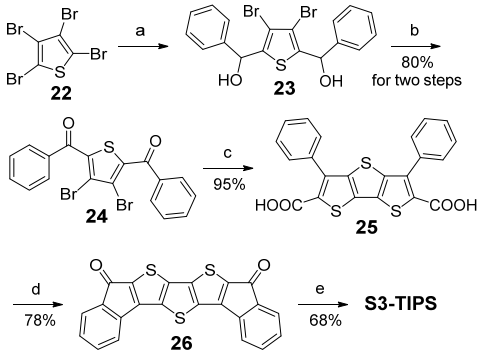

Scheme 3. Synthetic route of **S3-TIPS**: (a) i) *n*-BuLi, THF, -78 °C, 1 h; ii) PhCHO, -78 °C – r.t., overnight; (b) PCC, CH_2Cl_2, r.t., overnight; (c) i) HS-CH2COOEt, KOH, EtOH, r.t. for 2 h then 55 °C overnight; ii) KOH, EtOH, reflux, overnight; iii) 10% HCl (aq.); (d) i) $SOCl_2$, CH_2Cl_2, reflux; ii) $AlCl_3$, CH_2Cl_2, 0 °C – r.t., 12 h; (e) i) TIPSC≡CLi, THF, r.t., 12h; ii) $SnCl_2$, toluene, r.t., 12 h.

The synthesis of **S3-TIPS** was based on the key intermediate diketone **24**,[21] which was synthesized by a modified procedure in two steps from tetrabromothiophene (**22**) in an overall 80% yield (Scheme 3). Nucleophilic substitution and condensation reaction between **24** and ethyl mercaptoacetate followed by the hydrolysis of ester groups in the presence of potassium hydroxide afforded diacid **25** in 95% yield. Subsequent reactions following a similar protocol to that shown in Scheme 1 and Scheme 2 gave the target **S3-TIPS** in an overall 53% yield.

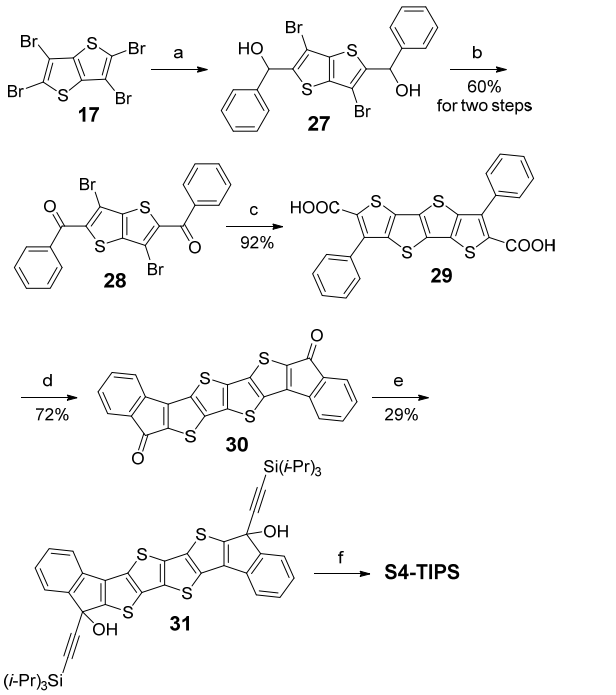

Scheme 4. Synthetic route of **S4-TIPS**: (a) i) *n*-BuLi, THF, -78 °C, 1 h; ii) PhCHO, -78 °C – r.t., overnight; (b) PCC, CH_2Cl_2, r.t., overnight; (c) i) HS-CH_2COOEt, KOH, EtOH, r.t. for 2 h then 55 °C overnight; ii) KOH, EtOH, reflux, overnight; iii) 10% HCl (aq.); (d) i) $SOCl_2$, CH_2Cl_2, reflux; ii) $AlCl_3$, CH_2Cl_2, 0 °C – r.t., 12 h; (e) TIPSC≡CLi, THF, r.t., 12h; f) $SnCl_2$, toluene, r.t., 30 min.

The synthesis of **S4-TIPS** utilized a similar strategy (Scheme 4). 2,3,5,6-Tetrabromothieno[3,2-b]thiophene (**17**) was treated with two equivalent *n*-butyllithium in THF solution at -78 °C followed by addition of benzaldehyde to give the diol **27**, which was then oxidized by pyridinium chlorochromate (PCC) to give the diketone **28** in 60% yield for two steps. The reaction of **28** with ethyl mercaptoacetate and potassium hydroxide in an ethanolic solution followed by addition of excess potassium hydroxide afforded the diacid **29** in one pot in 92% yield. Subsequent Friedel-Crafts acylation reaction afforded the diketone **30** in 72% yield. Nucleophilic addition of the diketone with lithiated TIPSE gave the diol **31** in 29% yield after column chromatography purification. Similar reduction of the diol **31** by $SnCl_2$ in different solvents (chloroform, toluene, THF etc.) under inert atmosphere gave the target compound **S4-TIPS**, which however is extremely reactive. The reaction was also conducted in deuterated solvents such as $CDCl_2CDCl_2$ under Ar and monitored by NMR spectrometry (Fig. S1 in ESI†). The reaction completed in 30 minutes with the formation of the desired **S4-TIPS**, which was confirmed by MALDI-TOF mass spectrometry (MS), but at the same time, side

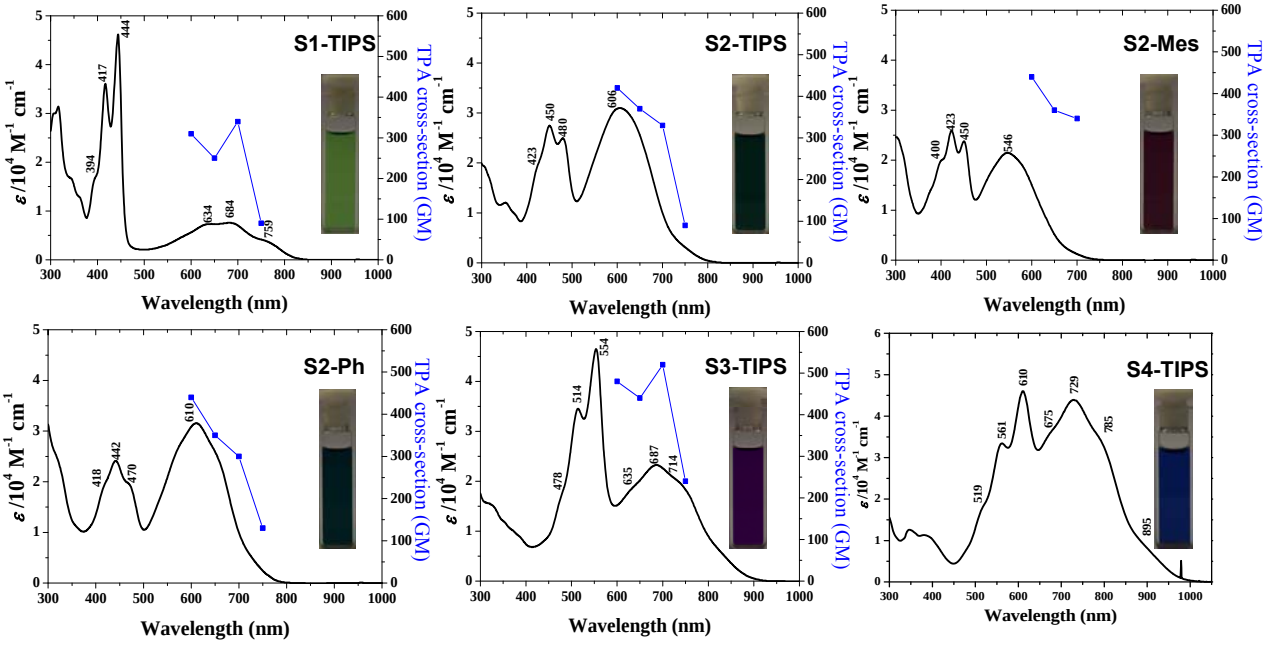

Fig. 2. One-photon absorption spectra (solid lines and left vertical axes) in $CHCl_3$ and two-photon absorption (TPA) spectra in toluene (blue symbols and right vertical axes) of **S1-TIPS**, **S2-TIPS**, **S2-Mes**, **S2-Ph**, **S3-TIPS** and **S4-TIPS**. TPA spectra are plotted at $\lambda_{ex}/2$. The TPA spectrum of **S4-TIPS** was not recorded due to its high reactivity. Insert are the photos of the solutions.

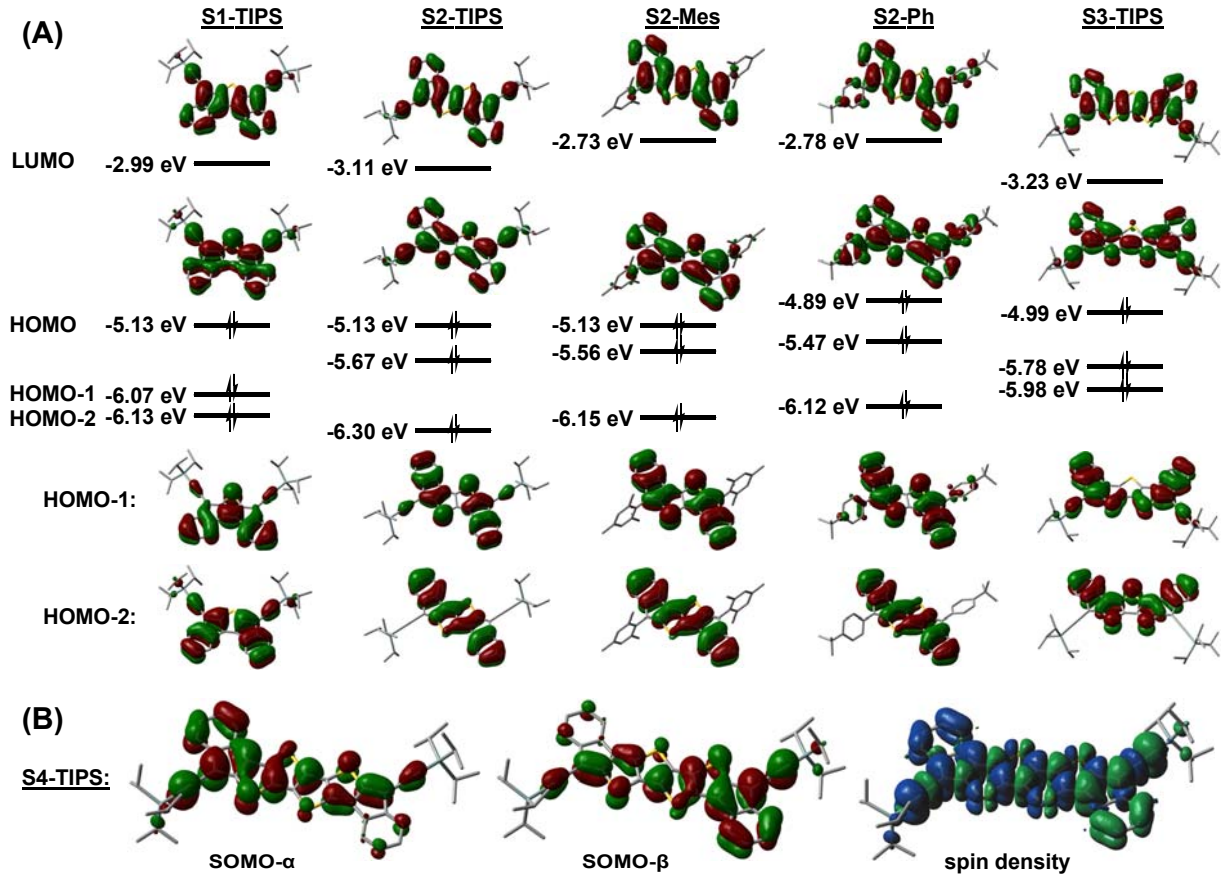

Fig. 3. (A) Calculated (B3LYP/6-31G**) frontier molecular orbital profiles and energy diagrams of **S1-TIPS**, **S2-TIPS**, **S2-Mes**, **S2-Ph** and **S3-TIPS**. (B) The calculated (UCAM-B3LYP/6-31G*) singly occupied molecule orbital profiles and spin density distribution of the singlet biradical of **S4-TIPS**.

Table 1 Summary of photophysical and electrochemical data

Compd.	λ_{abs} (nm)	ε (10^4 M^{-1} cm^{-1})	$E_{1/2}^{ox}$ (V)	$E_{1/2}^{red}$ (V)	HOMO (eV)	LUMO (eV)	E_g^{EC} (eV)	E_g^{opt} (eV)	τ (ps)	$\sigma^{(2)}_{max}$ (GM) (λ_{ex})
S1-TIPS	417	3.61	0.70	-1.62	-5.41	-3.69	1.72	1.51	1.9 (τ_1)	340
	444	4.62		-1.52					11 (τ_2)	(1400 nm)
	684	0.76		-1.21						
S2-TIPS	450	2.75	0.62	-1.42	-5.35	-3.75	1.60	1.58	1.1 (τ_1)	420
	480	2.50		-1.08					10 (τ_2)	(1200 nm)
	606	3.10								
S2-Mes	423	2.53	0.63	-1.39	-5.16	-3.64	1.62	1.71	1.2 (τ_1)	440
	450	2.38		-1.22					12 (τ_2)	(1200 nm)
	546	2.15								
S2-Ph	442	2.41	0.43	-1.52	-5.13	-3.82	1.52	1.58	1.1 (τ_1)	440
	470	1.98	0.84	-1.22					11 (τ_2)	(1200 nm)
	610	3.16								
S3-TIPS	514	3.45	0.40	-1.28	-5.30	-3.68	1.31	1.37	0.6 (τ_1)	520
	554	4.65	0.98	-1.02					7 (τ_2)	(1400 nm)
	687	2.33								
S4-TIPS	561	3.36[a]	-	-	-	-	-	1.27	-	-
	610	4.63[a]								
	729	4.41[a]								

λ_{abs}: absorption maxima. ε: molar extinction coefficient for the corresponding absorption maximum, [a] the ε values of **S4-TIPS** are extracted from the absorption spectrum after reaction for 34 min (Fig. S2 in ESI†), they should include minor errors and be smaller than the real values as **S4-TIPS** decomposes gradually during the experiments. $E_{1/2}^{ox}$ and $E_{1/2}^{red}$ are half-wave potentials of the oxidative and reductive waves, respectively, with potentials vs Fc/Fc^+ couple. HOMO = − (4.8 + E_{ox}^{onset}) and LUMO = − (4.8 + E_{red}^{onset}), where E_{ox}^{onset} and E_{red}^{onset} are the onset potentials of the first oxidative and reductive waves, respectively. E_g^{EC}: electrochemical band gap. E_g^{opt}: optical band gap estimated from the absorption onset. τ: singlet excited lifetime obtained from TA. $\sigma^{(2)}_{max}$: maximum TPA cross section. λ_{ex}: excitation wavelength in TPA measurements.

products formed. The reaction in dry toluene was also followed by UV-vis-NIR absorption spectroscopic measurements and similarly, the formation of the **S4-TIPS** was accompanied by simultaneous decomposition of the product (Fig. S2 in ESI†). Attempted separation of **S4-TIPS** by column chromatography or recrystallization all failed due to its high reactivity to oxygen, protonated reagents and silica gel, and complicated mixture mainly containing O_2-addition products were detected by MALDI-TOF MS (Fig. S3 in ESI†). Attempts to replace the TIPSE group by other bulky or electron-deficient aryl groups also failed to give stable compounds. The high reactivity of **S4-TIPS** is believed to be associated to its large biradical character (*vide infra*). Nevertheless, the sufficient lifetime ($t_{1/2}$ ~ 3h in N_2) allows us to probe its basic optical properties.

Electronic Absorption Spectropscopy

The steady-state OPA spectra of all the bisindeno-[*n*]theinoacenes are shown in Fig. 2 and the data are collected in Table 1. The frontier molecular orbital profiles, energy diagrams and the absorption spectra were also calculated by time-dependent (TD) DFT (B3LYP/6-31G*) (Fig. 3 and Fig. S4-S8 in ESI†). Two major bands were observed for all compounds. For **S1-TIPS**, the first intense band at 444 nm can be assigned to the HOMO-1→LUMO transition (f = 0.7393, 442.8 nm by TD DFT). The second weaker band at 684 nm is correlated to the HOMO→LUMO transition (f = 0.1511, 729.7 nm by TD DFT). Interestingly, such an electronic absorption spectrum is very similar to that of indeno[2,1-*c*]fluorene (**32**) derivative (Fig. 4).[10d] This is not surprising if we consider that the core of **S1-TIPS** is actually an isoelectronic structure of **32**, a dibenzannulated *as*-indacene. Similarly, compound **S3-TIPS** showed one intense band at 554 nm (HOMO-2→LUMO, f = 1.051, 530.7 nm by TD DFT) and one weaker band at 687 nm (HOMO→LUMO, f = 0.6399, 720.3 nm by TD DFT). The core of **S3-TIPS** can be regarded as an isoelectronic structure of the extended dibenzannulated *as*-indacene **34** (Fig. 4). The optical energy gap (E_g^{opt} = 1.37 eV) of **S3-TIPS** determined from the lowest energy absorption onset is smaller than **S1-TIPS** (E_g^{opt} = 1.51 eV) due to extended π-conjugation. Compounds **S2-TIPS**, **S2-Mes** and **S2-Ph** exhibited a different band structure from **S1-TIPS**/**S3-TIPS**, with one intense band at 450/423/442 nm (HOMO-2→LUMO) and one intense band at 606/546/610 nm (HOMO→LUMO), respectively. The band structure is somehow similar to the absorption spectrum of its isoelectronic structure fluoreno[4,3-*c*]fluorene (**33**), an extended dibenzannulated *s*-indacene (Fig. 4).[10e] The relatively larger optical band gap of **S2-TIPS** (E_g^{opt} =1.58 eV) compared to **S1-**

TIPS is interesting and could be related to the different fusion mode (*as*-indacene *vs. s*-indacene). Variation of the substituents has obvious effect on the absorption wavelength, but not on the band shape. In particular, the absorption maxima of **S2-Mes** shift significantly to higher energy side in comparison to **S2-TIPS** and **S2-Ph**. This can be attributed to the larger dihedral angle between the mesityl and bisindeno- thienothiophene core, which leads to diminished π-conjugation. This claim is evidenced by the X-ray crystallographic structures of **S2-Mes** (dihedral angle: 71.4°) and **S2-Ph** (dihedral angle: 36.2°) (*vide infra*). DFT calculations also showed that the HOMO and LUMO are less delocalized along the mesityl than 4-*tert*-phenyl unit (Fig. 3). The *in situ* generated **S4-TIPS** showed a similar band structure to **S2-TIPS**, which is reasonable considering that its isoelectronic structure **35** is an analogue of **33** (Fig. 4). The spectrum is however largely red-shifted. No fluorescence was observed for all compounds, indicating an ultrafast relaxation process of the excited state which is related to the antiaromaticity of these molecules. Looking into each electronic transition in more details (Fig. 3), the first absorption band at higher energy in these compounds can be correlated to the excitations within molecular orbitals mainly involving the external benzene rings and that are grouped in pairs of vibronic components of the same excitation (HOMO-1/HOMO-2→LUMO). The longer wavelength absorption band can be assigned to the transition mainly involving innermost antiaromatic indacene-thienoacene unit (HOMO→LUMO). It is worthy to highlight the longest wavelengths for the lowest energy lying absorptions of the smaller compounds (**S1-TIPS** and **S2-TIPS**) which is a spectroscopic signature of antiaromatic compounds.[22] This small gap also promotes very fast deactivation channels (e.g. vibrational relaxation) for the singlet excited state such as observed by the disappearance of fluorescence.

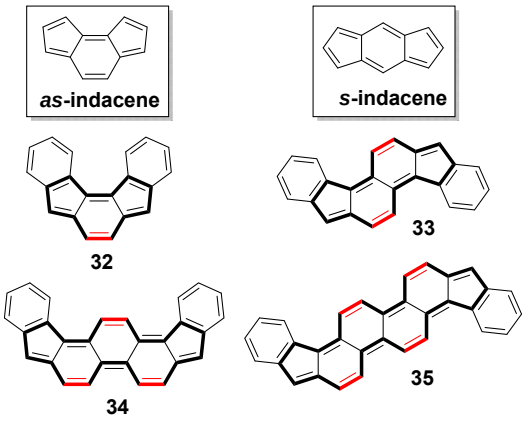

Fig. 4. Structures of *as*-/*s*- indacene and isoelectronic polycyclic hydrocarbons of **9**-**12**.

TA and TPA Measurements

Femtosecond TA measurements were utilized to explore the excited-state dynamics of **S1-TIPS**, **S2-TIPS**, **S2-Mes**, **S2-Ph** and **S3-TIPS** (Fig. 5 and Fig. S9 in ESI†). The TA spectrum of **S1-TIPS** displayed an intense excited-state absorption (ESA) band in a broad range of 450-750 nm. It did not show any perceptible ground-state bleach (GSB) signal due to the strong ESA contribution. The decay profiles probed at 505 nm were fitted by a double exponential function with the time constants of 1.9 and 11 ps (Table 1). Such a short singlet excited-state lifetime is in good agreement with its non-fluorescence nature.[23] The TA spectrum of **S2-TIPS** exhibited two distinct ESA bands at 490-540 nm/690-850 nm and two GSB bands that well match their steady-state absorption spectra. **S2-Mes** and **S2-Ph** displayed similar TA spectrum to that of **S2-TIPS** (Fig. S9 in ESI†). The singlet excited-state lifetimes of **S2-TIPS**, **S2-Mes** and **S2-Ph** were measured to be 10, 12 and 11 ps, respectively (Table 1), which are similar to that of **S1-TIPS**. The TA spectrum of **S3-TIPS** showed an intensive ESA band in the 570-650 nm along with two strong GSB signals in the 470-575 and 650-850 nm. Short singlet excited-state lifetime was also observed for **S3-TIPS** (~ 7 ps, Table 1). The short excited-state lifetimes observed for all compounds indicate an ultrafast relaxation process, which is a common phenomenon for most antiaromatic systems and singlet biradicaloids.[24, 11, 12]

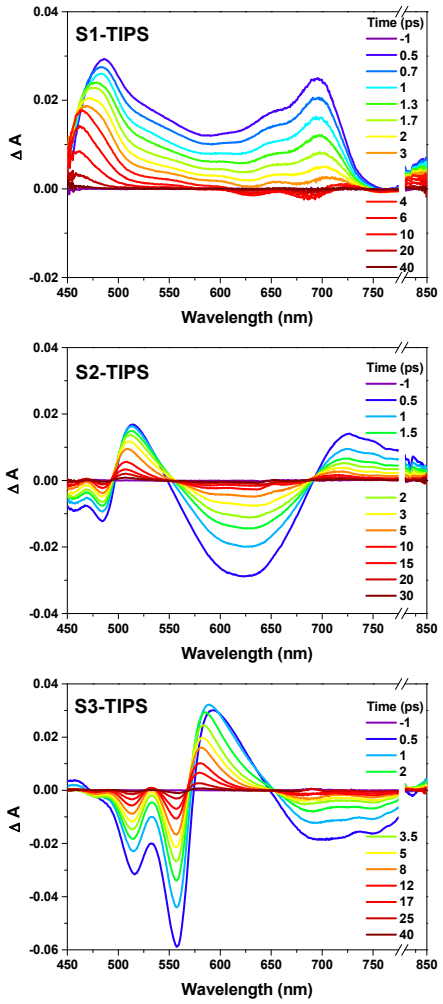

Fig. 5. Femtosecond transient absorption spectra of **S1-TIPS**, **S2-TIPS** and **S3-TIPS** measured in toluene with photoexcitation at 650, 650 and 700 nm, respectively.

TPA measurements were also conducted for **S1-TIPS**, **S2-TIPS**, **S2-Mes**, **S2-Ph** and **S3-TIPS** in toluene by Z-scan technique in the NIR region from 1200 to 1500 nm where one-photon absorption contribution is negligible (Fig. 2 and Fig. S10 in ESI†).[25] Owing to the extension of π-conjugation, the maximum TPA cross section values ($\sigma^{(2)}_{max}$) were increased from 340 GM (λ_{ex}: 1400 nm) for **S1-TIPS** to 420 GM (λ_{ex}: 1200 nm) for **S2-TIPS** and to 520 GM (λ_{ex}: 1400 nm) for **S3-TIPS**. The $\sigma^{(2)}_{max}$ values of **S2-Mes** and **S2-Ph** are similar to that of **S2-TIPS** (Table 1). Previous studies on singlet biradicaloids showed that chromophores with a small or moderate singlet biradical character usually exhibited strong third-order NLO response with large TPA cross sections.[26, 5, 11, 12] On the other hand, chromophores with an antiaromatic character usually display smaller TPA cross sections compared with the corresponding aromatic counterparts.[27] The observed moderate TPA cross sections can be explained by the unique property of our systems, that is, they can be regarded as antiaromatic systems which possess a small biradical character at the same time.

Ground-State Geometry and Electronic Structures

Single crystals suitable for X-ray crystallographic analysis were obtained for all final products except for **S4-TIPS** (due to its high reactivity) by slow diffusion of acetonitrile into $CHCl_3$ solution.[28] The Oak Ridge Thermal Ellipsoid Plot (ORTEP) drawings and 3D packing structures are shown in Fig. 6. The π-frameworks (bisindeno[*n*]thienoacene) of all the molecules are almost planar. **S1-TIPS** show a lamellar packing structure and in each layer, the molecules form a head-to-tail closely stacked polymer chain *via* π-π interactions between the bisindenothiophene cores (π-π distance: 3.41 Å). For **S2-TIPS**, two molecules form an anti-parallel packed

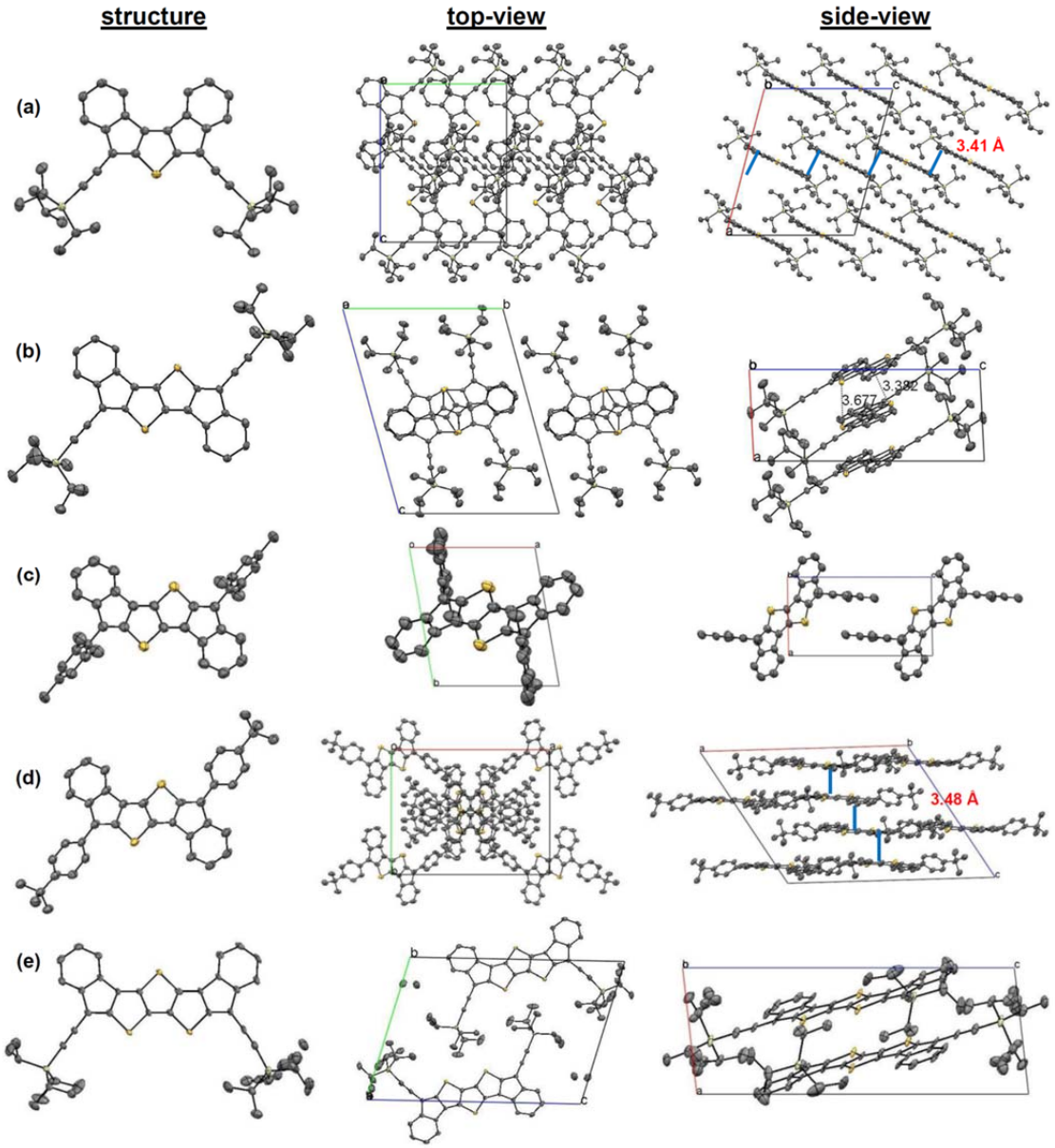

Fig. 6. X-ray crystallographic structures and packing structures of (a) **S1-TIPS**, (b) **S2-TIPS**, (c) **S2-Mes**, (d) **S2-Ph** and (e) **S3-TIPS**. Hydrogen atoms are omitted for clearance.

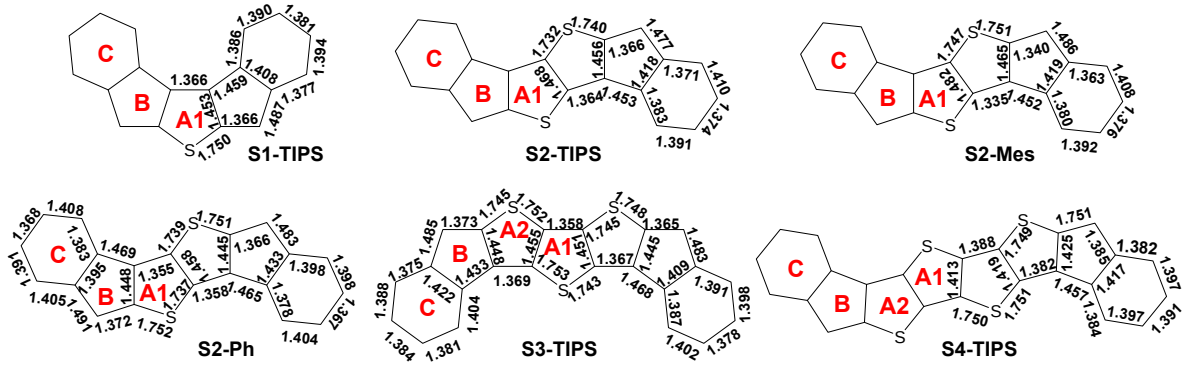

Fig. 7. Selected bond lengths for **S1-TIPS**, **S2-TIPS**, **S2-Mes**, **S2-Ph** and **S3-TIPS** from their crystallographic structures, and calculated bond lengths for the singlet biradical of **S4-TIPS**.

dimer *via* π-π interactions (distance: 3.382 Å) and [S···S] interactions (distance: 3.677 Å), which further stacks into a columnar structure. No π-stacking was observed for **S2-Mes** due to the bulky mesityl substituent. **S2-Ph** also showed a π-stacked columnar structure but with relatively large π-π distance (3.48 Å). No close π-stacking was observed for **S3-TIPS**. The observed close packing in **S1-TIPS**, **S2-TIPS** and **S2-Ph** indicated that they could serve as potential semiconductors in OFETs. Actually, our preliminary field effect transistor tests on the spin-coated thin films of **S2-TIPS** showed an average field effect hole mobility of 0.016 $cm^2V^{-1}s^{-1}$ in N_2 and 0.01 $cm^2V^{-1}s^{-1}$ in air (Fig. S11 and Table S6 in ESI†). Detailed device studies based on the spin-coated/vapor-deposited thin films and single crystals will be conducted in the future.

Bond length analysis was performed to better analyse the ground-state geometry (Fig. 7). In all cases, large bond length alternation was observed for the central biscyclopenta-thienoacene core, indicating a typical quinoidal structure with antiaromatic character. The outmost two benzene rings however showed less bond length alternation, indicating their large aromatic character.

DFT calculations (both UB3LYP/6-31G* and UCAM-B3LYP/6-31G*)[29] were conducted to understand the ground-state electronic structures. It was found that all the **S1-S3** series molecules indeed favor a closed-shell ground state. However, for **S4-TIPS**, the energy of its singlet biradical state is 4.0 and 3.6 kcal/mol lower than the triplet biradical and closed-shell state, respectively, thus suggesting a singlet biradical ground state. The calculated SOMO-α and SOMO-β profiles showed a disjoint character, with the spins evenly distributed along the whole π-conjugated framework (Fig. 3B). The singlet biradical character y_0 values were calculated as 0.03 for **S3-TIPS** and 0.202 (<S**2>= 0.8808) for **S4-TIPS**, while ignorable for **S1-TIPS** and **S2-TIPS**. Therefore, the singlet biradical character increases with the extension of chain length. The high reactivity of the **S4-TIPS** thus can be rationalized by its significant biradical character. The calculated geometry of the singlet biradical of **S4-TIPS** also showed large bond length alternation (Fig. 7), indicating that the quinoidal resonance form contributes most to the ground state.

Table 2. Calculated (UCAM-B3LYP/6-31G*) NICS(1)zz values for the rings A1-C of **S1-TIPS**, **S2-TIPS**, **S2-Mes**, **S2-Ph**, **S3-TIPS** and **S4-TIPS**. The rings are labeled in Fig. 7.

Compound	A1	A2	B	C
S1-TIPS	7.55	NA	15.93	-19.29
S2-TIPS	4.08	NA	10.11	-21.48
S2-Mes	3.46	NA	8.94	-22.06
S2-Ph	3.59	NA	9.58	-21.15
S3-TIPS	-2.10	0.16	10.07	-20.92
S4-TIPS	-6.63	-2.62	11.76	-19.90

Nucleus independent chemical shift (NICS) calculations were conducted to understand the trend of aromaticity of each ring (Fig. 7 and Table 2).[30] From **S1-TIPS** to **S4-TIPS**, the NICS(1)zz values for the central thiophene ring (ring A1) become more negative, indicating an increase of aromaticity with the extension of the chain length, which is in accordance with the increased biradical character. The cyclopenta-subunit (ring B) showed large positive NICS(1)zz values, indicating a typical antiaromatic character of central $4n$ π electron system, which is annulated and stabilized by two aromatic benzene rings (ring C) possessing large negative NICS(1)zz values. For **S3-TIPS** and **S4-TIPS**, the innermost thiophene ring (ring A1) is more aromatic than the neighbouring thiophene rings (ring A2).

In consistence with the change of the aromaticity and singlet biradical character with the extension of chain length, the ^{1}H NMR resonance peak for the proton *a* (see label in Fig. 1) showed graduate shift to the low-field from 7.13 ppm for **S1-TIPS** to 7.17 ppm for **S2-TIPS** and to 7.25 ppm for **S3-TIPS** (Fig. S12 in ESI†). Compound **S4-TIPS** exhibited broadened NMR spectrum at room temperature (Fig. S1 in ESI†) which could be ascribed to the existence of small amount of thermally excited triplet diradicals. ESR measurements on the *in situ* generated **S4-TIPS** in toluene showed a single-line ESR spectrum (g_e = 2.003) and the intensity decreases when temperature is lowered (Fig. S13 in

ESI†). This is a typical phenomenon for most systems with a singlet biradical ground state.[9-12] With the decrease of the temperature, the singlet-triplet equilibrium shifts to the lower energy singlet state, thus leading to a decrease of the magnetic susceptibility. Unfortunately, due to the difficulty to obtain pure sample, the exact singlet-triplet energy gap could not be determined by variable temperature ESR. **S4-TIPS** represents the largest size compound in which the destabilizing bounded electron pair (the highest energy pair of the 4*n* electrons) might get uncorrelated and, such as described for antiaromatic systems, would permit the formation of a highly unstable biradical species as confirmed by the data recorded for it.

Raman Spectroscopic Measurements

Raman spectroscopy has been proved to be a powerful tool to evaluate the electronic ground state and to understand macroscopic magnetic and optical data of π-conjugated systems.[3, 11-13] Therefore, the Raman spectra of **S1-TIPS**, **S2-TIPS** and **S3-TIPS** were recorded in powder form with different excitation wavelengths (Fig. 8). The Raman spectrum of **S1-TIPS** clearly highlights a strong bond-length alternation pattern with two intense bands dominating the spectrum at high frequencies values (denoting short C=C distances) at 1633 and 1525 cm^{-1} due to the C=C stretching modes, ν (C=C), of the cyclopentene double bonds and of the quinoidal thiophene, respectively. Quinoidal thiophene Raman bands typically appear close to 1400 cm^{-1}, a frequency value indicative of bond length equalization along the quinoidal conjugated path, in strong contrast with that at 1525 cm^{-1} in **S1-TIPS** revealing an accentuation of the bond length alternation pattern.[13d,13e]

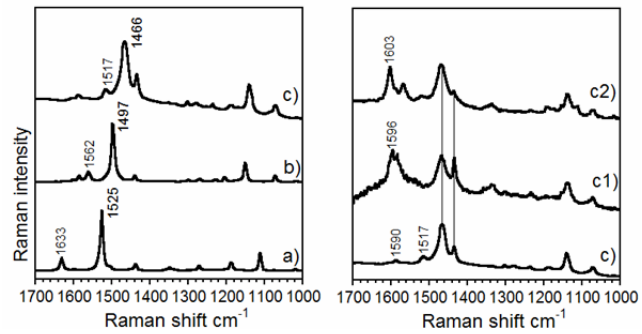

Fig. 8. Left: 1064 nm FT-Raman spectra of a) **S1-TIPS**, b) **S2-TIPS**, and c) **S3-TIPS**. Right: spectra of **S3-TIPS** taken with the excitation wavelengths at: c) 1064 nm, c1) 785 nm and c2) 532 nm.

The Raman spectra disclosed a very large change of the vibrational properties of the ground state as the dominating ν(C=C) bands move to lower frequencies at 1562/1497 and 1517/1466 cm^{-1} in **S2-TIPS** and **S3-TIPS**, respectively. This Raman behavior is consistent with a reduction of the bond length alternation pattern but still significantly expressed for **S2-TIPS** and **S3-TIPS**. Strong bond length alternation is a well-known property of even-parity antiaromatic systems as the inherent unstability provokes the ground state distortion towards a strongly C=C/C-C bond length alternated path. Besides the high frequency denoting a large bond length alternation, the concomitant decrease of the Raman frequencies is in agreement with a significant conjugation within the quinoidal thienoacene core. Going in Raman resonance with the main absorption bands of **S3-TIPS** at 516/553 nm (with the 532 nm laser Raman excitation) and at 686 nm (with the 785 nm Raman laser excitation), we observed the relative intensification of the 1600 cm^{-1} bands due to the largest involvement of the outermost benzenes in the whole antiaromatic path.

The Raman spectra of aromatic thienoacenes are characterized by the scarce variability of the strongest Raman bands as a function of the number of fused thiophene rings which is a consequence of the all-*cis* cross-conjugated disposition of the successive double bonds.[13] This behavior contrasts with that found in **S1-TIPS** – **S3-TIPS** series where a great dependence of the Raman bands is detected with the number of thiophene units which is in accordance with the persistence of the quinoidal forms in the thiophene rings in the three compounds. On the basis of the high ν (C=C) frequency values reflecting a large C=C/C-C bond alternation, **S1-TIPS** – **S3-TIPS** can also be formulated as thieno-quinoidal antiaromatic molecules with small biradical characters, which is in agreement with the above X-ray analysis and theoretical calculations.

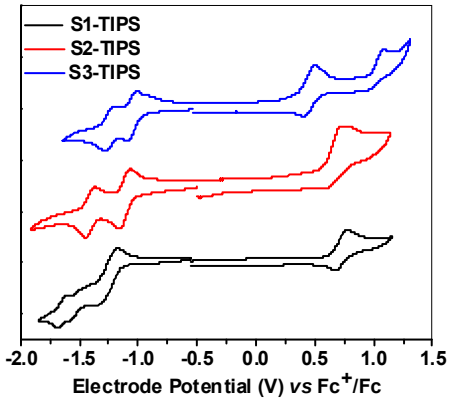

Fig. 9. Cyclic voltammograms of **S1-TIPS**, **S2-TIPS** and **S3-TIPS** in dry CH_2Cl_2 containing 0.1 M Bu_4NPF_6 as the supporting electrolyte, AgCl/Ag as the reference electrode, Au as the working electrode, Pt wire as the counter electrode, and a scan rate of 50 mV s^{-1}. The potential was externally calibrated against the ferrocene/ferrocenium redox couple.

Electrochemical and spectroelectrochemical studies

The electrochemical properties of **S1-S3** series were investigated by cyclic voltammetry in dry CH_2Cl_2 solution (Fig. 9, Table 1, and Fig. S14 in ESI†). All compounds showed amphoteric redox behavior with multiple (quasi-) reversible redox waves. **S1-TIPS** exhibited three reduction waves (half-wave potential $E_{1/2}^{red}$ = -1.62, -1.52, -1.21 V *vs* Fc^+/Fc) and one oxidation wave (half-wave potential $E_{1/2}^{ox}$ = 0.70 V *vs* Fc^+/Fc), indicating its high tendency to accept or loss electrons to form stable charged species. **S2-TIPS** displayed two reduction waves ($E_{1/2}^{red}$ = -1.42, -1.08 V) and one oxidation wave ($E_{1/2}^{ox}$ = 0.62 V), while **S3-TIPS** showed two reduction waves ($E_{1/2}^{red}$ = -1.28, -1.02 V) and two oxidation waves ($E_{1/2}^{ox}$ = 0.40, 0.98 V). The HOMO and LUMO energy levels were deduced from the onset potentials of the first oxidation (E_{ox}^{onset}) and the first reduction wave (E_{red}^{onset}), according to the following equations: HOMO = - (4.8 +

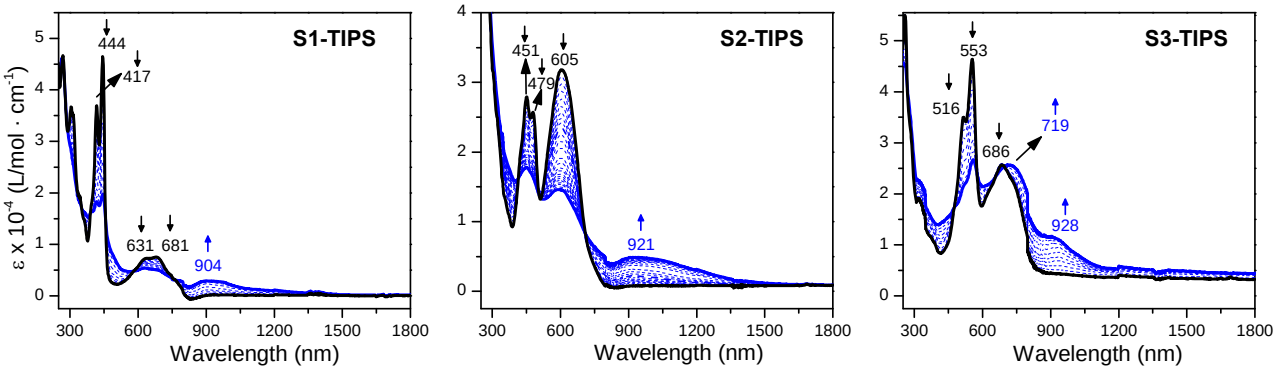

Fig. 10. UV-Vis-NIR absorption spectra of **Sn-TIPS** (n = 1, 2, 3) obtained during their potentiostatic oxidation in intervals of 50 mV. Blue lines: radical cation spectra.

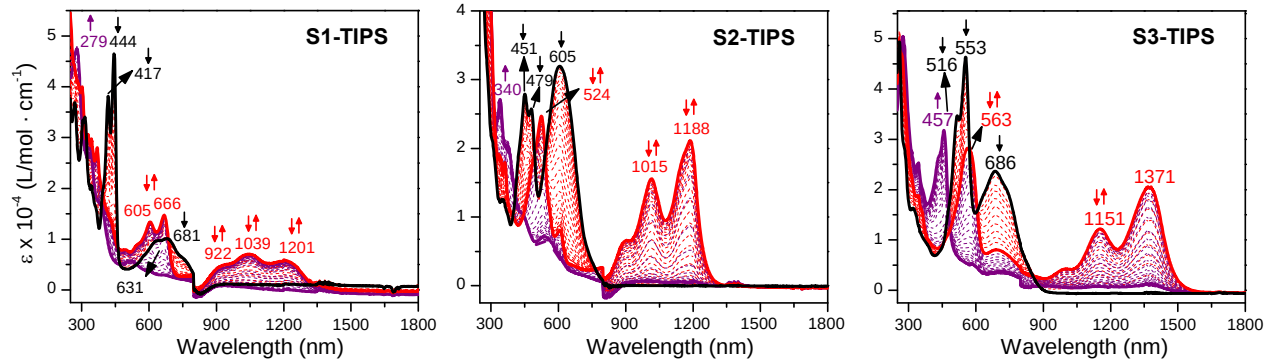

Fig. 11. UV-Vis-NIR absorption spectra of **Sn-TIPS** (n = 1, 2, 3) obtained during their potentiostatic reduction in intervals of 50 mV. Red line: radical anion spectra. Purple line: dianion spectra.

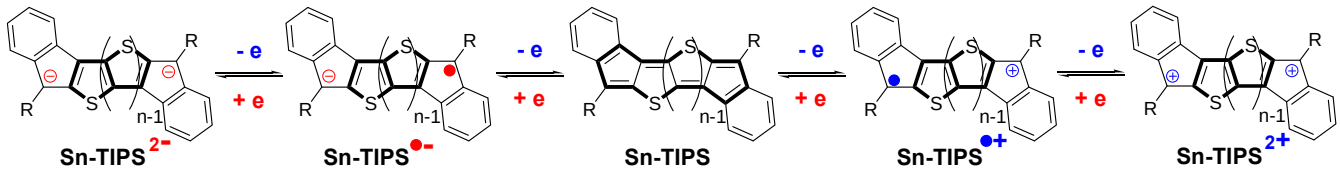

Scheme 5. Schematic presentation of the oxidation and reduction processes of **Sn-TIPS** (n = 1, 2, 3)

E_{ox}^{onset}) and LUMO = - (4.8 + E_{red}^{onset}), where the potentials are calibrated to $E(Fc^{+}/Fc)$ (Table 1). It was found that with the increase of π-conjugation from **S1-TIPS** to **S3-TIPS**, the electrochemical energy gaps (E_g^{EC}) decrease.

The multistage reversible redox waves and the large separation between the redox waves allow us to quantitatively attain the singly and doubly charged species by electrochemistry. UV-Vis-NIR spectroelectrochemical measurements were thus conducted for **S1-TIPS** – **S3-TIPS** in CH_2Cl_2 containing 0.1 M *n*-Bu_4NPF_6 as the supporting electrolyte by applying different electrode potentials and the absorption spectra were monitored by UV-vis-NIR spectrometer. For all three compounds, one electron extraction (oxidation) gave rise to the corresponding radical cations apparently characterized by two absorption bands (Fig. 10). The common feature is that the high energy absorption appeared in the high energy tail of the absorption band of the neutral compound, very close to it, being only well resolved in the case of **S3-TIPS** with a clear maximum at 719 nm. The second absorptions of these radical cations scarcely change with the molecular size, and are at 904, 921 and 928 nm for **S1-TIPS**, **S2-TIPS** and **S3-TIPS**, respectively. According to the antiaromatic framework, one electron extraction gives rise to a molecular species containing one aromatic thienoacene unit, one antiaromatic cyclopentadienyl cation, and one benzylic radical (Scheme 5), that is, the radical cations have a pseudo-aromatic character and are reasonably stable. Further oxidation is expected to give one aromatic thienoacene and two antiaromatic cyclopentadienyl cations (Scheme 5), which are thus unstable and difficult to attain by electrochemistry.

One-electron electrochemical reduction of the three neutral compounds gave rise to spectra characterized by two well differentiated groups of absorptions likely corresponding to two different excitations with vibronic structure (Fig. 11). One band appeared at the higher energy side of the neutral species (666/524/686 nm for **S1-TIPS**, **S2-TIPS** and **S3-TIPS**, respectively) and another band was observed at the lower energy side (1201/1188/1371 nm for **S1-TIPS**, **S2-TIPS** and **S3-TIPS**, respectively). The band shape and intensity are similar to those of many aromatic polycyclic hydrocarbons such as acenes[17] and

rylenes,[31] indicating an aromatic character of the radical anions. In fact, one-electron reduction should give one aromatic thienoacene unit, one aromatic cyclopentadienyl anion, and one benzylic radical (Scheme 5), which can explain the high stability of the radical anions. The second follow-up reduction gave rise to dianions with absorption spectra typical of aromatic thiophene and fused α-oligothiophenes,[15a-c] with absorption maximum at 279, 340 and 457 nm for **S1-TIPS**, **S2-TIPS** and **S3-TIPS**, respectively (Fig. 11). This reveals that for the dianions the structures have become fully aromatic within the thiophene rings, which can be easily elucidated by the formation of one aromatic thiophene/thienoacene unit and two aromatic cyclopentadienyl anions (Scheme 5). Our system provides a nice example of the competition between aromatic and antiaromatic cores and how they transform from one to the other depending on the number of added or extracted electrons.

Conclusions

In summary, a series of alkynyl or aryl substituted bisindeno-[*n*]thienoacenes (n = 1-4) were successfully synthesized *via* different strategies. This series of molecules can be regarded as antiaromatic systems with small singlet biradical characters. Their ground-state geometry and electronic structures were carefully studied by various experimental techniques (X-ray crystallographic analysis, NMR, ESR and Raman spectroscopy) and DFT calculations, and all of these data interpreted in the context of their antiaromaticity. It was found that with the extension of chain length the molecules showed gradually increased singlet biradical character and decreased antiaromaticity. In particular, the longest molecule **S4-TIPS** showed a singlet biradical ground state with a small-to-moderate biradical character (y_0 = 0.202). As a result, it displayed high reactivity. Their optical and electronic properties were systematically investigated by OPA, TPA, TA and cyclic voltammetry and revealed chain length dependent behavior. The observed short singlet excited state lifetime, moderate TPA cross section and amphoteric redox behavior all are related to their antiaromaticity and singlet biradical character. The transformation from antiaromatic to pseudo-aromatic/aromatic systems was conducted by electrochemical oxidation and reduction followed by UV-Vis–NIR spectroscopic measurements. Again, the aromaticity of the corresponding charged species can be used to well interpret their absorption spectra and stability. Our work provided the first study on a quinoidal thienoacene/polycyclic hydrocarbon hybrid system and disclosed the close relation between the antiaromaticity, singlet biradical character and their unique physical properties, which sheds light on the rational material design in the future.

Acknowledgements

C.C. acknowledges the financial support from MOE AcRF Tier 1 grants (R-143-000-510-112 and R-143-000-573-112) and NUS Start Up grant R-143-000-486-133. The work at the University of Málaga was supported by MINECO of Spain (CTQ2012-33733) and to the Junta de Andalucía (Project P09-FQM-4708). The work at Yonsei Univ. was supported by Mid-career Researcher Program (2010-0029668) and Global Research Laboratory (2013K1A1A2A02050183) through the National Research Foundation of Korea (NRF) funded by the Ministry of Science, ICT (Information and Communication Technologies) and Future Planning. K. H. acknowledges the financial support from KAUST.

Notes and references

[a] Department of Chemistry, National University of Singapore, 3 Science Drive 3, 117543, Singapore, E-mail: chmcc@nus.edu.sg
[b] Department of Physical Chemistry, University of Malaga, Campus de Teatinos s/n, 229071 Malaga, Spain, E-mail: casado@uma.es
[c] Department of Chemistry, Yonsei University, Seoul 120-749, Korea, E-mail: dongho@yonsei.ac.kr
[d] Institute of Materials Research and Engineering, A*STAR, 3 Research Link, 117602, Singapore
[e] Division of Physical Science and Engineering and KAUST Catalysis Center, King Abdullah University of Science and Technology (KAUST), Thuwal 23955-6900, Kingdom of Saudi Arabia, E-mail: kuowei.huang@kaust.edu.sa

Electronic Supplementary Information (ESI) available: [Synthetic procedures and characterization data for all new compounds, general experimental method, additional spectroscopic data, DFT calculation details, crystallographic data and OFET characerizations]. See DOI: 10.1039/b000000x/

(1) (a) J. L. Brédas and G. B. Street, *Acc. Chem. Res.,* 1985, **18**, 309; (b) L. M. Tolbert, *Acc. Chem. Res.,* 1992, **25**, 561; (c) T. Nishinaga, A. Wakamiya, D. Yamazaki and K. Komatsu, *J. Am. Chem. Soc.,* 2004, **126**, 3163; (d) D. Yamazaki, T. Nishinaga, N. Tanino and K. Komatsu, *J. Am. Chem. Soc.,* 2006, **128**, 14470; (e) M. Banerjee, S. V. Lindeman and R. Rathore, *J. Am. Chem. Soc.,* 2007, **129**, 8070; (f) M. Banerjee, R. Shukla and R. Rathore, *J. Am. Chem. Soc.,* 2009, **131**, 1780; (g) S. R. González, Y. Ie, Y. Sao, J. T. López Navarrete and J. Casado, *J. Am. Chem. Soc.,* 2011, **133**, 16350; (h) S. R. González, M. Carmen Tuiz Delgado, R. Caballero, P. De la Cruz, F. Langa, J. T. López Navarrete and J. Casado, *J. Am. Chem. Soc.,* 2012, **134**, 5675.

(2) See review articles: (a) Z. Sun and J. Wu, *J. Mater. Chem.,* 2012, **22**, 4151; (b) Z. Sun, Q. Ye, C. Chi and J. Wu, *Chem. Soc. Rev.,* 2012, **41**, 7857; (c) A. Shimizu, Y. Hirao, T. Kubo, M. Nakano, E. Botek and B. Champagne, *AIP Conf. Proc.,* 2012, **1504**, 399; (d) Z. Sun, Z. Zeng and J. Wu, *Chem. Asian J.,* 2013, **8**, 2894; (e) M. Abe, *Chem. Rev.,* 2013, **113**, 7011; (f) Z. Sun and J. Wu, *Pure Appl. Chem.,* 2014, DOI: 10.1515/pac-2013-1006.

(3) See review articles: (a) J. Casado, R. P. Ortiz and J. T. López Navarrete, *Chem. Soc. Rev.,* 2012, **41**, 5672; (b) J. Casado and J. T. López Navarrete, *Chem. Records,* 2011, **11**, 45.

(4) (a) M. Chikamatsu, T. Mikami, J. Chisaka, Y. Yoshida, R. Azumi and K. Yase, *Appl. Phys. Lett.,* 2007, **91**, 043506; (b) D. T. Chase, A. G. Fix, S. J. Kang, B. D. Rose, C. D. Weber, Y. Zhong, L. N. Zakharov, M. C. Lonergan, C. Nuckolls and M. M. Haley, *J. Am. Chem. Soc.,* 2012, **134**, 10349.

(5) K. Kamada, K. Ohta, T. Kubo, A. Shimizu, Y. Morita, K. Nakasuji, R. Kishi, S. Ohta, S.-I. Furukawa, H. Takahashi and M. Nakano, *Angew. Chem. Int. Ed.,* 2007, **46**, 3544.

(6) (a) Y. W. Son, M. L. Cohen and S. G. Louie, *Phys. Rev. Lett.,* 2006, **97**, 216803; (b) V. Dediu, L. E. Hueso, I. Bergenti and C. Tliani, *Nat. Mater.,* 2009, **8**, 707; (c) V. Dediu, L. E. Hueso and I. Bergenti, "Spin transport in organic semiconductors" (chapter 22) in the book, "Handbook of spin transport and magnetism", Taylor & Francis Group, 2012.

(7) (a) M. B. Smith and J. Michl, *Chem. Rev.,* 2010, **110**, 6891; (b) J. Lee, P. Jadhav, P. D. Reusswig, S. R. Yost, N. J. Thompson, D. N. Congreve, E. Hontz, T. Van Voorhis and M. Baldo, A. *Acc. Chem. Res.*, 2013, **46**, 1300.

(8) (a) Y. Morita, S. Nishida, T. Murata, M. Moriguchi, A. Ueda, M. Satoh, K. Arifuku, K. Sato and Takui, T. *Nat. Mater.,* 2011, **10**, 947; (b) J.-Y. Shin, T. Yamada, H. Yoshikawa, K. Awaga and H. Shinokubo, *Angew. Chem. Int. Ed.,* 2014, **53**, 3096.

(9) (a) K. Ohashi, T. Kubo, T. Masui, K. Yamamoto, K. Nakasuji, T. Takui, Y. Kai and I. Murata, *J. Am. Chem. Soc.,* 1998, **120**, 2018; (b) T. Kubo, M. Sakamoto, M. Akabane, Y. Fujiwara, K. Yamamoto, M. Akita, K. Inoue, T. Takui and K. Nakasuji, *Angew. Chem. Int. Ed.,* 2004, **43**, 6474; (c) T. Kubo, A. Shimizu, M. Sakamoto, M. Uruichi, K. Yakushi, M.

Nakano, D. Shiomi, K. Sato, T. Takui, Y. Morita and K. Nakasuji, *Angew. Chem. Int. Ed.,* 2005, **44**, 6564; (d) A. Shimizu, M. Uruichi, K. Yakushi, H. Matsuzaki, H. Okamoto, M. Nakano, Y. Hirao, K. Matsumoto, H. Kurata and T. Kubo, *Angew. Chem. Int. Ed.,* 2009, **48**, 5482; (e) A. Shimizu, T. Kubo, M. Uruichi, K. Yakushi, M. Nakano, D. Shiomi, K. Sato, T. Takui, Y. Hirao, K. Matsumoto, H. Kurata, Y. Morita and K. Nakasuji, *J. Am. Chem. Soc.,* 2010, **132**, 14421; (f) A. Shimizu, Y. Hirao, K. Matsumoto, H. Kurata, T. Kubo, M. Uruichi and K. Yakushi, *Chem. Commun.,* 2012, **48**, 5629.

(10) (a) D. T. Chase, B. D. Rose, S. P. McClintock, L. N. Zakharov and M. M. Haley, *Angew. Chem. Int. Ed.,* 2011, **50**, 1127; (b) A. Shimizu and Y. Tobe, *Angew. Chem. Int. Ed.,* 2011, **50**, 6906; (c) A. G. Fix, D. T. Chase and M. M. Haley, *Top. Curr. Chem.,* 2012, DOI: 10.1007/128_2012_376; (d) A. G. Fix, P. E. Deal, C. L. Vonnegut, B. D. Rose, L. N. Zakharov and M. M. Haley, *Org. Lett.,* 2013, **15**, 1362; (e) B. D. Rose, C. L. Vonnegut, L. N. Zakharov and M. M. Haley, *Org. Lett.*, 2013, **14**, 2426; (f) A. Shimizu, R. Kishi, M. Nakano, D. Shiomi, K. Sato, T. Takui, I. Hisaki, M. Miyata and Y. Tobe, *Angew. Chem. Int. Ed.,* 2013, **52**, 6076; (g) H. Miyoshi, S. Nobusue, A. Shimizu, I. Hisaki, M. Miyatab and Y. Tobe, *Chem. Sci.,* 2014, **5**, 163; (h) B. S. Young, D. T. Chase, J. L. Marshall, C. L. Vonnegut, L. N. Zakharov and M. M. Haley, *Chem. Sci.,* 2014, **5**, 1008.

(11) (a) R. Umeda, D. Hibi, K. Miki and Y. Tobe, *Org. Lett.,* 2009, **11**, 4104; (b) T. C. Wu, C. H. Chen, D. Hibi, A. Shimizu, Y. Tobe and Y. T. Wu, *Angew. Chem. Int. Ed.,* 2010, **49**, 7059; (c) Z. Sun, K.-W. Huang and J. Wu, *Org. Lett.,* 2010, **12**, 4690; (d) Z. Sun, K.-W. Huang and J. Wu, *J. Am. Chem. Soc.,* 2011, **133**, 11896; (e) Y. Li, W.-K. Heng, B. S. Lee, N. Aratani, J. L. Zafra, N. Bao, R. Lee, Y. M. Sung, Z. Sun, K.-W. Huang, R. D. Webster, J. T. López Navarrete, D. Kim, A. Osuka, J. Casado, J. Ding and J. Wu, *J. Am. Chem. Soc.,* 2012, **134**, 14913; (f) W. Zeng, M. Ishida, S. Lee, Y. Sung, Z. Zeng, Y. Ni, C. Chi, D.-H. Kim and J. Wu, *Chem. Eur. J.,* 2013, **19**, 16814; (g) Z. Sun, S. Lee, K. Park, X. Zhu, W. Zhang, B. Zheng, P. Hu, Z. Zeng, S. Das, Y. Li, C. Chi, R. Li, K. Huang, J. Ding, D. Kim and J. Wu, *J. Am. Chem. Soc.,* 2013, **135**, 18229; (h) Z. Sun and J. Wu, *J. Org. Chem.,* 2013, **78**, 9032; (i) L. Shan, Z.-X. Liang, X.-M. Xu, Q. Tang and Q. Miao, *Chem. Sci.,* 2013, **4**, 3294; (j) J. L. Zafra, R. C. González Cano, M. C. R. Delgado, Z. Sun, Y. Li, J. T. López Navarrete, J. Wu and J. Casado, *J. Chem. Phys.,* 2014, **140**, 054706; (k) Y. Li, K.-W. Huang, Z. Sun, R. D. Webster, Z. Zeng, W. D. Zeng, C. Chi, K. Furukawa and J. Wu, *Chem. Sci.,* 2014, **5**, 1908.

(12) (a) X. Zhu, H. Tsuji, H. Nakabayashi, S. Ohkoshi and E. Nakamura, *J. Am. Chem. Soc.,* 2011, **133**, 16342; (b) Z. Zeng, Y. M. Sung, N. Bao, D. Tan, R. Lee, J. L. Zafra, B. S. Lee, M. Ishida, J. Ding, J. T. López Navarrete, Y. Li, W. Zeng, D. Kim, K.-W. Huang, R. D. Webster, J. Casado and J. Wu, *J. Am. Chem. Soc.,* 2012, **134**, 14513; (c) Z. Zeng, M. Ishida, J. L. Zafra, X. Zhu, Y. M. Sung, N. Bao, R. D. Webster, B. S. Lee, R.-W. Li, W. Zeng, Y. Li, C. Chi, J. T. López Navarrete, J. Ding, J. Casado, D. Kim and J. Wu, *J. Am. Chem. Soc.,* 2013, **135**, 6363; (d) Z. Zeng, S. Lee, J. L. Zafra, M. Ishida, X. Zhu, Z. Sun, Y. Ni, R. D. Webster, R.-W. Li, J. T. López Navarrete, C. Chi, J. Ding, J. Casado, D. Kim and J. Wu, *Angew. Chem. Int. Ed.,* 2013, **52**, 8561; (e) Z. Zeng, S. Lee, J. L. Zafra, M. Ishida, N. Bao, R. D. Webster, J. T. López Navarrete, J. Ding, J. Casado, D. Kim and J. Wu, *Chem. Sci.* 2014, **5**, 3072.

(13) (a) V. Hernández, S. Calvo Losada, J. Casado, H. Higuchi and J. T. López Navarrete, *J. Phys. Chem. A,* 2000, **104**, 661; (b) J. Casado, T. M. Pappenfus, K. R. Mann, E. Ortí, P. M. Viruela, B. Milián, V. Hernández and J. T. López Navarrete, *ChemPhysChem,* 2004, **5**, 529; (c) T. Takahashi, K. I. Matsuoka, K. Takimiya, T. Otsubo, Y. Aso, *J. Am. Chem. Soc.,* 2005, **127**, 8928; (d) R. P. Ortiz, J. Casado, V. Hernandez, J. T. López Navarrete, P. M. Viruela, E. Orti, K. Takimiya and T. Otsubo, *Angew. Chem. Int. Ed*., 2007, **46**, 9057; (e) R. P. Ortiz, J. Casado, S. R. González, V. Hernández, J. T. López Navarrete, P. M. Viruela, E. Ortí, K. Takamiya and T. Otsubo, *Chem. Eur. J.,* 2010, **16**, 470; (f) E. V. Canesi, D. Fazzi, L. Colella, C. Bertarelli and C. Castiglioni, *J. Am. Chem. Soc.,* 2012, **134**, 19070.

(14) (a) T. M. Pappenfus, R. J. Chesterfield, C. D. Frisbie, K. R. Mann, J. Casado, J. D. Raff and L. L. Miller, *J. Am. Chem. Soc.,* 2002, **124**, 4184; (b) R. J. Chesterfield, C. R. Newman, T. M. Pappenfus, P. C. Ewbank, M. H. Haukaas, K. R. Mann, L. L. Miller and C. D. Frisbie, *Adv. Mater.,* 2003, **15**, 1278; (c) R. P. Ortiz, A. Facchetti, T. J. Marks, J. Casado, M. Z. Zgierski, M. Kozaki, V. Hernández, J. T and López Navarrete, *Adv. Funct. Mater.,* 2009, **19**, 386; (d) Y. Suzuki, E. Miyazaki and K. Takimiya, *J. Am. Chem. Soc.,* 2010, **132**, 10453.

(15) (a) X. Zhang, A. Côté and A. J. Matzger, *J. Am. Chem. Soc.,* 2005, **127**, 10502; (b) K. Xiao, Y. Liu, T. Qi, W. Zhang, F. Wang, J. Gao, W. Qiu, Y. Ma, G. Cui, S. Chen, X. Zhan, G. Yu, J. Qin, W. Hu and D. Zhu, *J. Am. Chem. Soc.,* 2005, **127**, 13281; (c) T. Okamoto, K. Kudoh, A. Wakamiya and S. Yamaguchi, *Chem. Eur. J.,* 2007, **13**, 548; (d) E.-G. Kim, V. Coropceanu, N. E. Gruhn, R. S. Sánchez-Carrera, R. Snoeberger, A. J. Matzger and J. L. Brédas, *J. Am. Chem. Soc.,* 2007, **129**, 13072; (e) K. Takimiya, S. Shinamura, I. Osaka and E. Miyazaki, *Adv. Mater.,* 2011, **23**, 4347; (f) A. N. Sokolov, S. Atahan-Evrenk, R. Mondal, H. B. Akkermanl, R. S. Sánchez-Carrera, S. Granados-Focil, S. Schrier, S. C. B. Mannsfeld, A. P. Zoombelt, Z. Bao and A. Aspuru-Guzik, *Nat. Commun.,* 2011, **2**, 437; (g) K. Niimi, S. Shinamura, I. Osaka, E. Miyazaki and K. Takimiya, *J. Am. Chem. Soc.,* 2011, **133**, 8732; (h) W. Xie, K. Willa, Y. Wu, R. Häusermann, K. Takimiya, B. Batlogg and C. D. Frisbie, *Adv. Mater.,* 2013, **25**, 3478; (i) T. Yokota, K. Kuribara, T. Tokuhara, U. Zschieschang, H. Klauk, K. Takimiya, Y. Sadamitsu, M. Hamada, T. Sekitani and T. Someya, *Adv. Mater.,* 2013, **25**, 3639.

(16) (a) K. Yui, H. Ishida, Y. Aso, T. Otsubo, F. Ogura, A. Kawamoto and J. Tanaka, *Bull. Chem. Soc. Jpn.,* 1989, **62**, 1547; (b) Q. Wu, R. Li, W. Hong, H. Li, X. Gao and D. Zhu, *Chem. Mater.,* 2011, **23**, 3138.

(17) (a) J. E. Anthony, *Chem. Rev.,* 2006, **106**, 5028; (b) J. E. Anthony, *Angew. Chem. Int. Ed.,* 2008, **47**, 452; (c) H. Qu, C. Chi, *Curr. Org. Chem.,* 2010, **14**, 2070.

(18) A. Henckens, K. Colladet, S. Fourier, T. J. Cleij, L. Lutsen, J. Gelan and D. Vanderzande, *Macromolecules,* 2005, **38**, 19.

(19) L. S. Fuller, B. Iddon and K. A. Smith, *J. Chem. Soc., Perkin Trans. 1*, 1997, 3465.

(20) (a) X. Shi, J. Chang and C. Chi, *Chem. Commun.,* 2013, **49**, 7135; (b) T. Kunz and P. Knochel, *Chem. Eur. J.,* 2011, **17**, 866.

(21) D. T. Tùng, D. T. Tuân, N. Rasool, A. Villinger, H. Reinke, C. Fischer and P. Langer, *Adv. Synth. Cat.,* 2009, **351**, 1595.

(22) (a) F. Dietz, N. Tyutyulkov and M. Rabinovitz, *J. Chem. Soc. Perkin Trans. 2*, 1993, 157; (b) F. Dietz, M. J. Rabinovitz, A. Tadjer and N. Tyutyulkov, *J. Chem. Soc. Perkin Trans. 2*, 1995, 735.

(23) J. Lakowicz, *Principles of Fluorescence Spectroscopy*, Kluwer Academic/Plenum Publishers, New York, Boston, Dordrecht, London, Moscow, 1999.

(24) (a) E. M. Giacobbe, G, Q. Mi, M. T. Colvin, B. Cohen, A. Ramana, A. M. Scott, S. Yeganeh, T. J. Marks, M. A. Ratner and M. R. Wasielewski, *J. Am. Chem. Soc*., 2009, **131**, 3700; (b) K. Ishii, Y. Hirose, H. Fujitsuka, O. Ito and N. Kobayashi, *J. Am. Chem. Soc.,* 2001, **123**, 702.

(25) M. Sheik-Bahae, A. A. Said, T.-H. Wei, D. J. Hagan and E. W. Van Stryland, *IEEE J. Quant. Electr.,* 1990, **26**, 760. Our TPA set-up is 1200-2400nm, and the maximum TPA cross-section values cannot be assigned.

(26) M. Nakano, R. Kishi, A. Takebe, M. Nate, H. Takahashi, T. Kubo, K. Kamada, K. Ohta, B. Champagne aned E. Botek, *Comput. Lett.,* 2007, **3**, 333.

(27) (a) M. Pawlicki, H. A. Collins, R. G. Denning and H. L. Anderson, *Angew. Chem. Int. Ed.,* 2009, **48**, 3244; (b) T. K. Ahn, J. H. Kwon, D. Y. Kim, D. W. Cho, D. H. Jeong, S. K. Kim, M. Suzuki, S. Shimizu, A. Osuka and D. Kim, *J. Am. Chem. Soc.,* 2005, **127**, 12856; (c) Y. Tanaka, S. Saito, S. Mori, N. Aratani, H. Shinokubo, N. Shibata, Y. Higuchi, Z. S. Yoon, K. S. Kim, S. B. Noh, J. K. Park, D. Kim and A. Osuka, *Angew. Chem. Int. Ed.,* 2008, **47**, 681; (d) J. M. Lim, Z. S. Yoon, J.-Y. Shin, K. S. Kim, M.-C. Yoon and D. Kim, *Chem. Commun.,* 2009, 261.

(28) (a) Crystallographic data for **S1-TIPS**: $C_{40}H_{50}SSi_2$, M = 619.04, monoclinic, a = 18.8584(12) Å, b = 12.3701(8) Å, c = 15.9959(11) Å, α = 90°, β = 104.724(4)°, γ = 90°; V = 3609.0(4) Å^3, T = 153(2) K, space group C2/c, Z = 4, CuKα radiation λ = 1.54178 Å, 11612 reflections measured, 3024 independent reflections (*Rint* = 0.0481). The final R_1 values were 0.0532 ($I > 2\sigma(I)$). The final $wR(F^2)$ values were 0.1386 ($I > 2\sigma(I)$). The final R_1 values were 0.0685 (all data). The final $wR(F^2)$ values were 0.1511 (all data). The goodness of fit on F^2 was 1.091. CCDC number: 1004903. (b) Crystallographic data for **S2-TIPS**: $C_{42}H_{50}S_2Si_2$, M = 675.14, triclinic, a = 7.402(6) Å, b = 14.535(11) Å, c = 18.955(14) Å, α = 73.693(15)°, β = 83.913(16)°, γ = 77.680(14)°, V = 1910(3) Å^3, T = 123(2) K, space group P-1, Z = 2, CuKα radiation λ = 1.54178 Å, 26316 reflections measured, 7205 independent reflections (*Rint* = 0.2133). The final R_1 values were 0.0719 ($I > 2\sigma(I)$). The final $wR(F^2)$ values were 0.1581 ($I > 2\sigma(I)$). The final R_1 values were 0.1814 (all data). The final $wR(F^2)$ values were 0.2103 (all data). The goodness of fit on F^2 was 0.996. CCDC number: 1004904. (c) Crystallographic data for **S2-Mes**: $C_{38}H_{30}S_2$, M = 550.76, triclinic, a = 7.0732(12) Å, b = 7.9974(14) Å, c = 12.843(2) Å, α = 83.771(13)°, β = 88.008(13)°, γ = 79.973(14)°, V = 711.1(2) Å^3, T =

173(2) K, space group P-1, Z = 1, CuKα radiation λ = 1.54178 Å, 9077 reflections measured, 2144 independent reflections (*Rint* = 0.1118). The final R_1 values were 0.0811 ($I > 2\sigma(I)$). The final $wR(F^2)$ values were 0.2103 ($I > 2\sigma(I)$). The final R_1 values were 0.1262 (all data). The final $wR(F^2)$ values were 0.2501 (all data). The goodness of fit on F^2 was 1.017. CCDC number: 1004905. (d) Crystallographic data for **S2-Ph**: $C_{40}H_{34}S_2$, M = 578.79, monoclinic, a = 24.0560(10) Å, b = 16.0276(10) Å, c = 18.3518(16) Å, $\alpha = 90^o$, $\beta = 122.105(4)^o$, $\gamma = 90^o$, V = 5993.7(7) Å^3, T = 123(2) K, space group C2/c, Z = 8, CuKα radiation λ = 1.54178 Å, 24423 reflections measured, 5317 independent reflections (*Rint* = 0.2779). The final R_1 values were 0.1245 ($I > 2\sigma(I)$). The final $wR(F^2)$ values were 0.3045 ($I > 2\sigma(I)$). The final R_1 values were 0.1843 (all data). The final $wR(F^2)$ values were 0.3754 (all data). The goodness of fit on F^2 was 1.156. CCDC number: 1004906. (e) Crystallographic data for **S3-TIPS**: $C_{44}H_{50}S_3Si_2$, M = 731.20, triclinic, a = 7.5100(3) Å, b = 14.0747(6) Å, c = 20.3192(9) Å, $\alpha = 73.205(2)^o$, $\beta = 81.761(2)^o$, $\gamma = 82.646(2)^o$, V = 2026.41(15) Å^3, T = 153(2) K, space group P-1, Z = 2, CuKα radiation λ = 1.54178 Å, 14925 reflections measured, 6144 independent reflections (*Rint* = 0.0760). The final R_1 values were 0.0974 ($I > 2\sigma(I)$). The final $wR(F^2)$ values were 0.2475 ($I > 2\sigma(I)$). The final R_1 values were 0.1142 (all data). The final $wR(F^2)$ values were 0.2663 (all data). The goodness of fit on F^2 was 1.047. CCDC number: 1004907.

(29) (a) T. Yanai, D. Tew and N. Handy, *Chem. Phys. Lett.,* 2004, **393**, 51; (b) R. Seeger and J. A. Pople, *J. Chem. Phys.,* 1977, **66**, 3045.

(30) H. Fallah-Bagher-Shaidaei, C. S. Wannere, C. Corminboeuf, R. Puchta and P.v.R, Schleyer, *Org. Lett.,* 2006, **8**, 863.

(31) T. Weil, T. Vosch, J. Hofkens, K. Peneva and K. Müllen, *Angew. Chem. Int. Ed.,* 2010, **49**, 9068.